Ecosystems
https://doi.org/10.1007/s10021-019-00463-w

Ecosystem Nitrogen Response to a Simulated Ice Storm in a Northern Hardwood Forest

Julie N. Weitzman,[1,2,9]* Peter M. Groffman,[1,2,3] John L. Campbell,[4] Charles T. Driscoll,[5] Robert T. Fahey,[6] Timothy J. Fahey,[7] Paul G. Schaberg,[8] and Lindsey E. Rustad[4]

[1]*City University of New York Advanced Science Research Center at the Graduate Center, New York, New York, USA;* [2]*Cary Institute of Ecosystem Studies, Millbrook, New York, USA;* [3]*Department of Earth and Environmental Sciences, Brooklyn College, New York, New York, USA;* [4]*Northern Research Station, USDA Forest Service, Durham, New Hampshire, USA;* [5]*Department of Civil and Environmental Engineering, Syracuse University, Syracuse, New York, USA;* [6]*Department of Natural Resources and the Environment & Center for Environmental Sciences and Engineering, University of Connecticut, Storrs, Connecticut, USA;* [7]*Department of Natural Resources, Cornell University, Ithaca, New York, USA;* [8]*Northern Research Station, USDA Forest Service, Burlington, Vermont, USA;* [9]*Present address: Present Address: ORISE Fellow at U.S. Environmental Protection Agency, Western Ecology Division, Ecological Effects Branch, Corvallis, Oregon, USA*

Abstract

Ice storms are important but understudied disturbances that influence forest structure and function. In 1998, an ice storm damaged forest canopies and led to increased hydrologic losses of nitrogen (N) from the northern hardwood forest at the Hubbard Brook Experimental Forest (HBEF), a Long-Term Ecological Research (LTER) site in New Hampshire, USA. To evaluate the mechanisms underlying this response, we experimentally simulated ice storms with different frequencies and severities at the small plot scale. We took measurements of plant and soil variables before (2015) and after (2016, 2017) treatments using the same methods used in 1998 with a focus on hydrologic and gaseous losses of reactive N, as well as rates of soil N cycle processes. Nitrogen cycle responses to the treatments were insignificant and less marked than the responses to the 1998 natural ice storm. Pools and leaching of inorganic N, net and gross mineralization and nitrification and denitrification rates, and soil to atmosphere fluxes of nitrous oxide (N_2O) were unaffected by the treatments, in contrast to the 1998 storm which caused marked increases in leaching and watershed export of inorganic N. The difference in response may be a manifestation of N oligotrophication that has occurred at the HBEF over the past 30 years. Results suggest that ecosystem response to disturbances, such as ice storms, is changing due to aspects of global environmental change, challenging our ability to understand and predict the effects of these events on ecosystem structure, function, and services.

Key words: climate change; denitrification; disturbance; mineralization; nitrate; nitrification; nitrogen; nitrous oxide.

Received 2 August 2019; accepted 3 November 2019

Authors' Contributions: JNW performed the research, was involved in collecting, analyzing, and interpreting the bulk of the data, and drafted the manuscript with PMG, with input from all the authors. PMG provided mentoring to JNW throughout the study. JLC, RTF, and LER contributed additional data and interpretation. PMG, JLC, CTD, TJF, PGS, and LER secured funding and conceived of the study. All authors provided critical feedback for revision of the final manuscript.

**Corresponding author; e-mail:* WeitzmanJ@caryinstitute.org

Published online: 21 November 2019

Highlights

- There was little short-term response of the forest N cycle to simulated icing events.
- This limited response contrasted with a 1998 natural ice storm, which resulted in elevated N losses.
- The response of the HBEF to disturbance is changing due to a shift toward oligotrophy.

Introduction

Ecosystem response to disturbance is an enduringly important and challenging topic in ecosystem ecology (Pickett and White 1983; Ratajczak and others 2018). Although it is clear that disturbance is an inherent factor in all ecosystems, variation in the nature, extent and intensity of disturbance events, and the complexity of ecosystem response has limited the development of overarching principles to guide research as well as our ability to make useful predictions quantifying ecosystem response and recovery (Turner 2010; Peters and others 2011). As societal concerns about the value and preservation of ecosystem services grow, the need for a comprehensive understanding and predictive capacity of the occurrence of disturbance and associated ecological response has become increasingly acute (Grimm and others 2013).

Many disturbance studies have focused on biogeochemical response variables (Bormann and Likens 1979; Kranabetter and others 2016). Fluxes of water and nutrients respond dynamically to disturbance. Quantifying these responses can be facilitated by the widely used watershed approach in ecosystem science (Likens 2013). There has been a particular focus on nitrogen (N) as a biogeochemical response variable due to its importance to ecosystem productivity, the presence of highly reactive and mobile forms that readily respond to disturbance, and concerns about the delivery of this element to receiving waters and the atmosphere where it can impair water and air quality, respectively (Vitousek and others 1979; Galloway and others 2003).

Multiple aspects of global environmental change have complicated analysis of ecosystem response to disturbance. Not only is the frequency and intensity of extreme climatic events increasing (Wuebbles and others 2014), but more chronic changes in climate, atmospheric chemistry, and community composition have altered ecosystem response to these events. These changes are evident in biogeochemical responses, which can be highly sensitive to changes in temperature, precipitation, atmospheric deposition of N, sulfur (S) and acidity, and levels of atmospheric carbon dioxide (CO_2) (Durán and others 2016; Niu and others 2016; Sabo and others 2016).

Ice storms are a regionally important, but understudied, type of disturbance (Changnon 2003). They can have particularly severe impacts on forests, as ice accumulation can alter canopy structure, leaf area, and photosynthetic capacity leading to changes in the demand for and fluxes of water and nutrients (Rhoads and others 2002; Lafon 2004; Weeks and others 2009). Production of inorganic N (mineralization and nitrification) can continue unchanged or shift following disturbance, which, when coupled with a change in plant demand, alters the pool of inorganic N available for export (Vitousek and others 1982). Hydrologic and gaseous losses of N can be moderated by increases in processes that consume (immobilization, denitrification) or conserve (mineralization) inorganic N that can be stimulated by inputs of carbon (C) from damaged plant canopies to the soil (Hart and others 1994a; Morse and others 2015b).

A severe ice storm impacted northeastern North America in January 1998, resulting in significant increases in export of dissolved inorganic N from forested watersheds at the Hubbard Brook Experimental Forest (HBEF) for 2 years (Houlton and others 2003). These losses appeared to be driven by decreases in plant demand for N, as there was no increase in soil production of inorganic N, and ceased once leaf area index returned to pre-disturbance levels (Houlton and others 2003). However, there was significant variation in N leaching response within and among watersheds that was driven by land use history, species composition, and the nature and extent of C input from the damaged canopy to the soil (Houlton and others 2003). The regional nature and high impact of the 1998 ice storm heightened interest in these events as an important area of research in regions where ice storms are common (Gyakum and Roebber 2001; Rustad and Campbell 2012). There is also evidence that the frequency of ice storms is increasing, a pattern that may continue under a future changing climate (Cheng and others 2007; Hayhoe and others 2007; Cheng and others 2011).

To resolve mechanistic uncertainties about forest ecosystem response to ice storms and to develop a more predictive understanding of their impact, an experimental ice storm manipulation experiment was initiated at the HBEF. Using methods developed in a preliminary experiment (Rustad and

Campbell 2012), we varied the frequency and severity of icing to the overstory canopy on replicated plots and took detailed measurements of plant and soil variables before (2015) and after (2016, 2017) treatment. A major focus of the measurements was on soil N cycle processes (mineralization, nitrification, and denitrification; Groffman and others 2009) and hydrologic and gaseous losses of reactive N (Yanai and others 2013). Ancillary measurements of plant response to treatment and C fluxes (soil respiration, coarse and fine litterfall, root growth; Fahey and others 2005) were taken to provide context for the N measurements. The objectives of this study were to: (1) evaluate ecosystem N cycle response to variation in ice storm frequency and severity in the northern hardwood forest, with a focus on hydrologic and gaseous losses; (2) compare the nature and extent of these losses with observations of the response to the 1998 ice storm; and (3) understand mechanisms underlying variation in response within and among treatments and between the 1998 natural and 2016/2017 experimental storms.

Materials and Methods

Study Site and Experimental Design

The HBEF Long-Term Ecological Research (LTER) site is an approximately 3200-ha northern hardwood forest situated in the southern part of the White Mountain National Forest, New Hampshire, USA (43°56′N, 71°45′W). Exhibiting a continental temperate climate typical of the Northeast, the HBEF experiences long, cold winters and short, mild to cool summers. The HBEF has a mean air temperature of − 9°C in January versus 18°C in July and has a mean annual precipitation of about 1400 mm y^{-1} of which one-third to one quarter typically occurs as snow. The soils of the HBEF are dominated by shallow (75–100 cm), acidic (pH 3.9–4.5), well-drained Spodosols (Typic Haplorthods) with sandy loam textures derived from unsorted glacial till. Though relatively infertile, the soils currently support a second-growth forest of even-aged vegetation, of which about 80–90% is hardwoods and 10–20% conifers.

The ice storm manipulation experiment (ISE) was established in an area of the HBEF consisting of 70–100–year-old mixed hardwood stands near the main branch of the Hubbard Brook (Figure 1A). The dominant and co-dominant crown class tree species in the study plots are red maple (*Acer rubrum*), sugar maple (*Acer saccharum*), and yellow birch (*Betula alleghaniensis*). This area was chosen for its proximity to a water source (the main branch of the Hubbard Brook) and its similarity in vegetation species composition, soil type, and land use history (non-agricultural) to watershed 1 (W1) and watershed 6 (W6) at the HBEF, which were the main sites investigated for ecosystem response to the 1998 ice storm study (Houlton and others 2003). Ten plots of 20 × 30 m (Figure 1B) were established in summer 2015, and pre-treatment measurement collections were initiated. The rectangular shape and size of the plots made it possible to fully ice the crowns of trees in the interior of plots using equipment placed along the outside edges. Each of the ten main plots was further gridded into 5 × 5 m subplots for sampling purposes. Three levels of subplots were assigned as follows: (1) internal subplots; eight subplots within the inner 10 × 20 m of the main plot; (2) intensive subplots; a random selection of four of the eight internal subplots for intensive process measurements; and (3) buffer subplots; 16 subplots surrounding the inner 10 × 20 m internal subplots, which provided a 5-m buffer zone to reduce edge affects. Two main plots were randomly assigned to each of the following five icing treatments of varying intensities (0–19 mm ice accretion) and frequency (one icing event per year for 1 or 2 years): (1) reference; no experimental icing applied, that is, 0 mm; (2) low; 6.4 mm of ice in year 1 only; (3) mid; 12.7 mm of ice in year 1 only; (4) mid × 2; 12.7 mm of ice in year 1 and year 2; and (5) high; 19.0 mm of ice in year 1 only. The targeted amounts of ice accretion for the treatments were chosen to be relevant to National Weather Service Ice Storm Warnings in the northeastern USA, which occur for icing events of 0.25 in (6.4 mm) for states of the mid-Atlantic region and 0.5 in (12.7 mm) for New York and the New England states. Ice accretion during the 1998 ice storm was highly variable and increased with elevation, but had measured ice thickness ranges similar to those targeted in this study (Rustad and Campbell 2012). Radial ice thickness measured on tree branches across the area affected by the natural ice storm of 1998 ranged from 5.9 mm at low elevation (< 625 m) to 14.4 mm at high elevation (709–791 m) (Rhoads and others 2002; Rustad and Campbell 2012).

The ice storm simulations occurred during subfreezing conditions across five different dates in 2016 on January 18, January 27–29, and February 11, 2016 (due to there being 8 plots total to spray), for year 1 and on January 14, 2017 (as there were only two plots to spray), for year 2. Streamwater, which has a low ionic strength similar to the

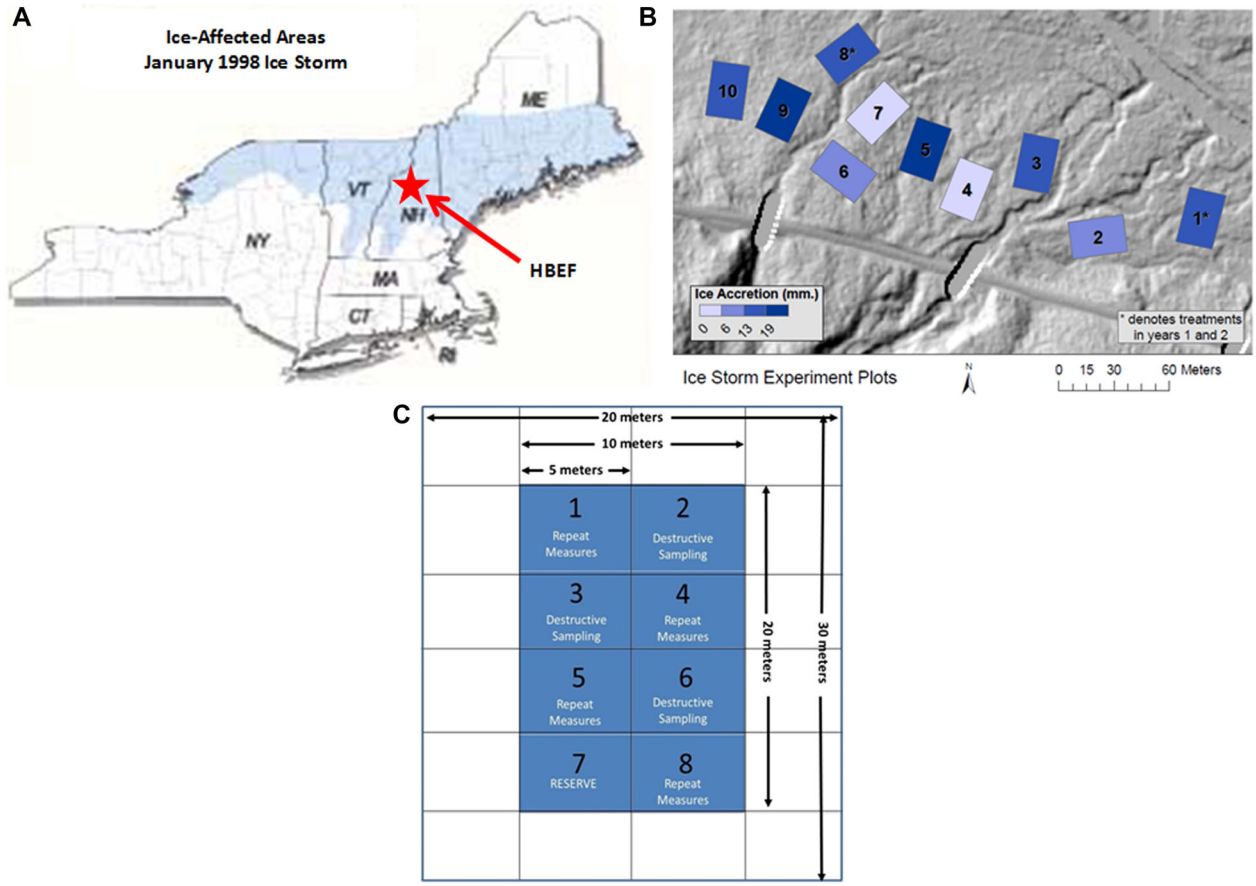

Figure 1. **A** Map of the Hubbard Brook Experimental Forest (HBEF), a Long-Term Ecological Research (LTER) site, located in the White Mountains of New Hampshire. The blue color indicates the ice-affected areas across the states of New York (NY), Vermont (VT), New Hampshire (NH), and Maine (ME) following the 1998 ice storm (adapted from Miller-Weeks and others 1999). **B** Arrangement of the ten 20 × 30 m sampling plots near the main branch of Hubbard Brook, with treatments indicated by the blue color gradient. **C** Subplots within each of the ten 20 × 30 m sampling plots (Color figure online).

ambient precipitation that falls on the HBEF, was applied by pumping water from the main branch of the Hubbard Brook using BB4® centrifugal pumps (that is, portable firefighting equipment) attached to hoses with nozzles mounted on tracked vehicles that were driven back and forth along paths on the longer sides of each plot. Water was sprayed evenly over the canopy so that it descended as a fine mist and froze on contact with trees. Targeted ice accretion amounts were achieved in the field by periodically making measurements during water application with calipers on tree branches that were within reach. Ice accretion, reported as equivalent radial ice thickness (the thickness of ice that would be measured if the actual ice accretion on a branch was of uniform thickness), was determined using wooden dowel ''ornaments'' suspended in the canopy. These methods were shown to be effective approaches for gauging ice accretion in a 2011 pilot study (Rustad and Campbell 2012).

Hydrologic Losses

Soil solutions were collected fortnightly with 2.1 × 9.5 cm length porous cup tension lysimeters (Prenart Equipment ApS, Frederiksberg, Denmark) installed in the B soil horizon in four subplots in each plot (that is, four lysimeters per plot). Each soil lysimeter was plumbed to a 1-l glass sample bottle housed in a 15-cm-diameter polyvinyl chloride (PVC) tube that was buried vertically 50 cm in the ground with a cap at the surface. Tension (30 kPa) was applied with a vacuum hand pump the day before samples were collected. Because the bottles were stored underground, the water samples remained in a cool, dark environment during the collection period and did not freeze during winter. The lysimeters were installed in spring 2015, which allowed 4 months for equilibration in the soil before the beginning of the study period in fall 2015.

Soil water samples were stored frozen until analysis at the USDA Forest Service Laboratory in Durham, New Hampshire, which occurred within a maximum of 1 month after they were collected from the field. Concentrations of NO_3^- were measured with ion chromatography (Metrohm 761, Herisau, Switzerland), NH_4^+ with automated colorimetry (SmartChem 200 Discrete Analyzer, Westco Scientific Instruments, Inc., Brookfield, Connecticut, USA), and total dissolved N (TDN) with high-temperature catalytic combustion and chemiluminescent N detection (Shimadzu TOC-VCSH/TNM-1 analyzer, Shimadzu Scientific Instruments, Inc., Columbia, Maryland, USA). Dissolved organic N (DON) was determined as the difference between TDN and dissolved inorganic N ($NO_3^- + NH_4^+$).

Fluxes of NO_3^-, NH_4^+, DON, and TDN from the B horizon were calculated using modeled daily soil water determined with the BROOK90 hydrologic model (Federer 2017). BROOK90 simulates water movement through multiple soil layers, making it possible to approximate the flux of soil water from different horizons. The model was run using daily minimum and maximum temperature (average of measurements at two locations at the ISE plots), precipitation from rain gauge 19 ($\sim$ 0.7 km from the ISE plots), and vapor pressure, solar radiation, and wind speed measured at the Robert S. Pierce Ecosystem Laboratory at the HBEF ($\sim$ 4.6 km from the ISE plots). Changes in transpiration associated with canopy damage were not considered in the model; therefore, the same soil water leaching volume was simulated across all treatments. However, any transpiration effects would be small, as leaching occurs primarily during the dormant season. Daily fluxes were calculated by multiplying the daily chemical concentration (mg l^{-1}) by the daily soil water flux (mm day^{-1}) for that day. Daily chemical concentrations between sampling dates were determined by linear interpolation between soil solution collections. Daily fluxes were then summed to monthly and annual values. Given that we used the same soil water leaching volume for all treatments, any differences are solely due to differences in measured concentrations in leachate. However, we reported fluxes rather than concentrations to facilitate comparison with other measured flux values (for example, nitrification, mineralization, gas flux).

Soil Sampling

Soil samples were collected and N cycle processes were measured 5–7 times (varying among assays) over a span of 3 years (2015–2017). All analyses, described in detail below, were carried out one time prior to any icing (that is, pre-treatment in fall 2015) and at least four times following the year 1 icing event (that is, post-treatment in spring and fall 2016 and 2017), with the exception of in situ nitrous oxide (N_2O) gas flux measurements (two pre-treatment and three post-treatment collections) and in situ denitrification rate (that is, gas fluxes of di-nitrogen, N_2, and N_2O from intact cores) measurements (zero pre-treatment and four post-treatment collections). Some post-treatment measurements of N cycling process rates were also taken in summer 2016 and 2017.

Pre-treatment Sampling

In August and September 2015 (pre-treatment), soils were collected from each of the ten established plots to determine baseline values for a number of different soil properties. All soil samples were collected using split, sharpened PVC cores of 5 cm diameter $\times$ 15 cm depth. On August 26, 2015, six paired soil cores were removed from each of the ten established plots, which equated to two paired replicates from three randomly selected subplots within each plot. Six of the cores (two replicates of each pair from each of three subplots) were sealed in polyethylene bags and immediately re-inserted into the ground for in situ incubation according to the buried bag method (see below for more details). The other six cores (two replicates of each pair from each of three subplots) were returned intact to the laboratory, separated into organic and mineral soil horizons, and the horizons were homogenized by hand (removing roots and rocks when present, which were weighed and measured for volume). Subsamples of the fine earth material were then removed for laboratory analysis of gravimetric water content, ''initial'' inorganic N concentrations, potential net N mineralization, potential net nitrification, and potential denitrification (see below for specific details of each analysis). To allow for enough soil material for organic matter analysis, soil from the two replicates from each subplot was composited for each soil horizon. Organic matter was measured on composite samples of the two replicates from each subplot for each soil horizon by loss on ignition (LOI) over 4 h at 450°C (below the temperature where carbonate materials can be volatilized) (Salonen 1979; Nelson and Sommers 1996; Santisteban and others 2004).

On 23 September 2015, the cores incubating in situ were removed from the field, soil horizons were split and homogenized, and each subplot

replicate was once again subsampled for analysis of gravimetric water content and ''final'' inorganic N concentrations. In situ net N mineralization and net nitrification rates were then calculated (see below for details). On the same day, another set of soil samples was collected for determination of gross N cycle process rates (see below). Within each of the ten plots, six soil cores were removed, with two replicates taken from three randomly selected subplots in each plot. The organic and mineral soil horizons were split in the field for each sample, and the two replicates for each subplot were composited. Soils were returned to the laboratory, homogenized by hand, and gross N transformations were assessed via the ^{15}N isotope dilution method (see below).

Soil to atmosphere fluxes of N_2O were measured in September and October 2015, prior to the icing events. Specifically, in situ concentrations of N_2O were measured by collecting soil gas from four static gas sampling chambers placed at the soil surface in each of the ten ISE plots, utilizing the in situ chamber design described by Bowden and others (1991) (see below).

Bulk Density

Bulk density for both the organic and mineral horizons of each of the ten ISE plots (accounting for previously removed rocks) was estimated from the pre-treatment organic matter content, based on an empirical relationship developed for forest soils on coarse-textured till in the New England region of the USA (Federer and others 1993). Over a large range of organic fractions, the relationship follows equation (1):

$$D_b = \frac{D_{bm} D_{bo}}{F_o D_{bm} + (1 - F_o) D_{bo}} \quad (1)$$

where D_b is the bulk density, D_{bm} is the bulk density of ''pure'' mineral matter (equal to 1.45 Mg m^{-3} for the soils of the HBEF), D_{bo} is the bulk density of ''pure'' organic matter (equal to 0.111 Mg m^{-3} for the soils of the HBEF), and F_o is the measured organic fraction. Calculated bulk densities for the three subplots within each plot were then averaged for each of the two soil horizons to estimate bulk density values for each specific plot. From these calculated bulk density values and measured average horizon thicknesses across the plots (4.7 cm for the organic soil horizon and 10 cm for the mineral soil horizon), C and N concentrations and process rates were expressed on an areal basis for each plot. Plot mean values were used in statistical analyses to avoid concerns about pseudoreplication.

Post-treatment Sampling

Soil N cycling processes were measured in each plot for two consecutive years after the manipulation, in the spring and fall of 2016 and 2017 (with some measurements also taken in the summers) following the year 1 icing application in 2016. The post-treatment soil sampling scheme was similar to that described for pre-treatment analyses, with the only difference being the number of replicates within each subplot. For laboratory analysis of gravimetric water content, initial inorganic N concentrations, potential net N mineralization, potential net nitrification, and potential denitrification, three replicates in each of three subplots were collected, split by horizon, and composited in the field. Only one core in each of the same three subplots was incubated in situ and later removed for determination of in situ net N mineralization and nitrification rates. Sampling for gross N cycling rates, however, remained the same as pre-treatment collections—two replicates in each of three subplots were split by horizon in the field and the two replicates were then composited. Collection of soils for determination of gross N cycling rates always occurred when the in situ incubating cores were removed from the field, while sampling for the other N cycling variables occurred at both the time of burial and the time of removal of in situ incubating cores (hence the addition of summer observations for these variables).

Measurement of in situ denitrification rates (that is, gas fluxes of N_2 and N_2O from intact cores) via the nitrogen-free air recirculation method (N-FARM) (Burgin and others 2010; Burgin and Groffman 2012; Morse and others 2015a; Morse and others 2015b) occurred only post-treatment and required the collection of another set of soil samples for analysis. One paired set of intact cores was collected in the spring and fall of 2016 and 2017 from a randomly selected subplot in each of the experimental plots and returned to the laboratory. One core in each pair was used to estimate in situ denitrification rates, while the other core was destructively sampled for determination of potential net N mineralization and nitrification rates. These samples were not split into their respective soil horizons, and the potential rates are based on homogenized samples that contained a mix of organic and mineral soil material.

Post-treatment sampling for in situ N_2O gas fluxes at the soil surface followed the same proce-

dure as that of pre-treatment gas sampling, with gas collected from four static gas sampling chambers within each of the ten ISE plots, and occurred once in August 2016 and once in both July and October 2017.

Microbial N Transformations

In Situ Potential Net N Mineralization and Potential Net Nitrification

Net N mineralization and net nitrification were measured using the in situ buried bag method (Matson and Vitousek 1981; Knoepp and Swank 1995; Robertson and others 1999; Durán and others 2012) in fall 2015 (pre-treatment) and spring and fall 2016 and 2017 (post-treatment). At the start of each incubation period, 5 cm diameter × 15 cm depth intact cores were removed from each plot (the number of cores removed was dependent on whether the sampling occurred pre-treatment or post-treatment—see above). A set of cores were returned intact to the laboratory, split into organic and mineral soil horizons, and the horizons were homogenized by hand (removing roots and rocks). From each soil horizon, a subsample was analyzed for gravimetric water content (dried in a forced-air oven at 60°C for 48 h) and another subsample was analyzed for ''initial'' inorganic N [ammonium (NH_4^+) and nitrate (NO_3^-)] after immediate extraction for 1 h with 2 M potassium chloride (KCl). Inorganic N concentrations were quantified colorimetrically using a Lachat Quick Chem 8100 Flow Injection Analyzer (Lachat Instruments, Milwaukee, Wisconsin, USA). The other cores from the paired sets were sealed in polyethylene bags and immediately re-inserted into the ground for in situ incubation. The cores were incubated for approximately 4–8 weeks before removal, and the above laboratory analyses were repeated. In situ net N mineralization and net nitrification rates were calculated as the accumulation of total inorganic N ($NH_4^+ + NO_3^-$) and NO_3^- alone, respectively, over the course of the field incubation.

Laboratory Potential Net N Mineralization and Potential Net Nitrification

Potential net N mineralization and potential net nitrification rates were assessed using 10-day laboratory incubations (Binkley and Hart 1989; Hart and others 1994b; Hart and Stark 1997). From split and homogenized soil samples collected at the time of burial (pre-treatment and post-treatment) and another set collected at the time of removal of in situ incubating cores (post-treatment only), subsamples were immediately extracted with 2 M KCl and analyzed for ''initial'' inorganic N concentrations as described above. At the same time, a separate set of subsamples were placed in Mason jars and incubated for ten days, after which they were extracted in 2 M KCl, and their inorganic N concentrations measured. As described above for in situ rates, laboratory potential net N mineralization and potential net nitrification rates were quantified from the accumulation of total inorganic N and NO_3^-, respectively, during the 10-day incubation.

Laboratory Potential Denitrification

Potential denitrification (denitrification enzyme activity, DEA) was measured using the short-term anaerobic assay developed by Smith and Tiedje (1979), as described by Groffman and others (1999). Split and homogenized soils from fall 2015 and spring, summer and fall 2016 and 2017 were amended with potassium nitrate (KNO_3^-), dextrose, chloramphenicol (to inhibit synthesis of new enzymes), and acetylene and were incubated under anaerobic conditions for 90 min. Samples were made anaerobic by repeated evacuation and flushing with N_2 gas. Gas samples were collected at 30 and 90 min, stored in evacuated glass tubes, and analyzed for N_2O by electron capture gas chromatography on a Shimadzu GC-2014 (Shimadzu Scientific Instruments, Inc., Columbia, Maryland, USA). Potential denitrification was calculated from the change in N_2O concentration over the 90-min incubation period. Total gas evolved included the N_2O dissolved in water estimated using the Bunsen's coefficient (Young 1981) at incubation temperature, corrected for headspace and water volume.

Gross N Mineralization and Nitrification

Gross N transformations were measured using a ^{15}N pool dilution technique in short-term laboratory incubations of organic and mineral soil samples (Hart and others 1994b; Groffman and others 2006; Christenson and others 2009). To estimate the gross rate of N mineralization, a tracer-level addition of aqueous $^{15}NH_4Cl$ (ammonium chloride, 99 atom % ^{15}N enriched, ~ 3 mg N per kg dry soil) was sprayed directly onto 80 g of field moist soil spread in a thin layer in a metal baking pan. Once the labeled solution was added, the sample was thoroughly mixed and divided into four subsamples of similar weight (approximately 20 g each). Two of the subsamples were extracted immediately (that is, within 15 min) with 2 M KCl. These sub-

samples served as method replicates and provided a measure of the initial NH_4^+ pool (Davidson and others 1991). The remaining two subsamples were placed in 120-ml plastic specimen cups, covered with plastic wrap, incubated at room temperature for 72 h (following Venterea and others 2004), and extracted with 2 M KCl following the incubation period. This same procedure was carried out to determine the gross rate of nitrification, expect $^{15}KNO_3$ (potassium nitrate, 98 atom % ^{15}N enriched, ~ 3 mg N per kg dry soil) was added instead of $^{15}NH_4Cl$.

Following extraction, all samples were analyzed for inorganic N via flow injection analysis, as described above. The respective isotopic ratios of ^{15}N and ^{14}N in NH_4^+ and NO_3^- in the samples before and after incubation were quantified at the U.C. Davis Isotope Laboratory from prepared diffused acidified disks (Stark and Hart 1996). The N-diffusion method (Stark and Hart 1996) is used to concentrate inorganic N from soil extracts onto diffused traps prior to total N and ^{15}N enrichment analysis by continuous flow direct combustion-mass spectrometry. Blank solutions, as well as spiked solutions with known enrichment and N mass, were diffused along with samples in order to obtain an estimate of the quantity of N contamination, and extraction efficiency, respectively, allowing a correction factor to be applied to samples.

The equations of Kirkham and Bartholomew (1954) as presented in Hart and others (1994a, b), which use data on $^{14+15}N$ and ^{15}N in the initial and incubated soil samples, and pool sizes of labeled pools, were used to calculate gross rates of N mineralization (here ammonification), nitrification, NH_4^+ immobilization, and NO_3^- immobilization. Gross N immobilization was calculated as total inorganic N immobilization ($NH_4^+ + NO_3^-$) minus gross nitrification.

Soil/Atmosphere Fluxes of Nitrous Oxide

Surface gas fluxes of N_2O were measured using an in situ chamber design (Bowden and others 1991). Static gas soil sampling chambers (four per plot) of 20-cm-diameter (ID) PVC were placed on permanently installed PVC base rings immediately prior to measurement. At 0-, 10-, 20-, and 30-min following placement of the chamber on the base, 8-ml gas samples were collected from gas sampling ports in the center of the chamber top by syringe. Samples were transferred to evacuated glass vials and stored at room temperature prior to N_2O analysis by electron capture gas chromatography as described above. Surface fluxes of N_2O were calculated from the linear rate of change in gas concentration, the chamber internal volume, and soil surface area. Flux rate calculations were not corrected for actual in situ temperature and pressure.

Intact Core Denitrification Rates

Denitrification was estimated by measuring fluxes of N_2 and N_2O from intact soil cores incubated in gastight chambers in an N-FARM measurement system. Prior to the start of incubations, a 16-h period of alternating vacuum/flush cycles (every 90 s) removed background atmospheric N_2 from the chamber headspaces, replacing it with a mixture of 20% oxygen (O_2) and 80% ultra-high purity helium (He). Soils were incubated for 4–6 h in this N_2-free atmosphere, and the concentrations of N_2 and N_2O in the headspace of each chamber were measured at three times (generally 0, 2–3, and 4–6 h) using a Shimadzu GC-2014 (Shimadzu Scientific Instruments, Inc., Columbia, Maryland, USA) in-line with the N-FARM system. In situ denitrification rates are presented as the net production of N_2O and N_2 during the N-FARM incubation period, while N_2O yield is calculated as the percentage of N_2O produced in relation to total denitrification [that is, $N_2O/(N_2O + N_2)$].

Statistical Analysis

Differences in soil N cycling processes with icing treatment and sampling date were evaluated using the general linear model function, which is a proxy for repeated-measures analysis of variance (ANOVA), in Minitab 17.1 (Minitab Inc., State College, Pennsylvania, USA). Residuals were checked for assumptions of normality, homoscedasticity, and outliers and data-transformed when necessary prior to analyses. Icing treatment amount, sample date, and their interaction were treated as main factors, while plot replicate was included as a random factor effect. When main effects or interactions were found to be significant ($P < 0.05$), data were further analyzed by a one-way ANOVA, and Tukey's HSD post hoc test (with 95% confidence limits) was used to compare differences.

Soil solution N data were evaluated with a generalized linear mixed model fit with residual pseudolikelihood estimation (GLIMMIX procedure in SAS 9.4; SAS Institute, Inc. Cary, North Carolina, USA). Treatment effects were analyzed on monthly fluxes of NO_3^-, NH_4^+, DON, and TDN using a repeated-measures randomized complete block design, and annual means after treatment (2016 and 2017) were compared with contrasts. Icing

treatment amount, sample time (month), and their interaction were treated as fixed effects, and plot replicate as a random effect. A gamma distribution (log link function) was selected for the model because it yielded the best fit among candidate distributions. A first-order, autoregressive covariance structure was used to account for temporal autocorrelation. Denominator degrees of freedom were adjusted with the Kenward–Roger approximation. All post hoc analyses were performed with a Tukey–Kramer test, and differences were considered significant at $\alpha = 0.05$.

Results

There was little response of the N cycle to the icing treatments, with no significant differences in the rapid, dynamic response variables of the N cycle (that is, leaching losses, NO_3^- pools, net nitrification rates, and N_2O production rates) over the 2-year post-treatment sampling period. Sample date did not have significant effects on these N cycling variables, nor did icing treatment amount or frequency. Therefore, results are presented as averages of time, treatments, or both, to better visualize patterns. Gross rates of N mineralization, N immobilization, nitrification, and NO_3^- immobilization, however, showed significant differences with time, but not with treatment, for both the organic and mineral horizons. For method comparison purposes, gross rates of N mineralization and nitrification were averaged across all times and treatments for each soil horizon (Table 1). Significant differences across time for all gross rates are presented (with treatments averaged) and discussed separately.

Hydrologic N Losses

Soil solution losses of inorganic N ($NO_3^- + NH_4^+$) in all icing treatments were low, less than 0.04 g N m^{-2} y^{-1} (Table 2). Soil solution losses of TDN ranged from 0.13 to 0.31 g N m^{-2} y^{-1} across years and treatments and were largely associated with DON (range = 57–95%, median = 90% of TDN). Statistical analyses of monthly fluxes of all forms of N in soil solution leaching from the B horizon showed no significant response to experimental icing during the 2 years after treatment (NO_3^-, $P = 0.401$; NH_4^+, $P = 0.635$; DON, $P = 0.347$; TDN, $P = 0.361$). The effect of time was significant (NO_3^-, $P < 0.001$; NH_4^+, $P < 0.001$; DON, $P < 0.001$; TDN, $P = 0.019$), indicating differences in monthly fluxes that were associated with seasonal trends and hydrologic events (for example, snowmelt). For NO_3^- and NH_4^+, there was a significant treatment–time interaction (NO_3^-, $P < 0.001$; NH_4^+, $P = 0.038$), but no clear pattern in the response. Mean monthly fluxes of NH_4^+ were significantly higher ($P = 0.001$) during the second year after the ice was applied (2017) compared to the first year (2016), suggesting enhanced mineralization across all treatments in 2017. All the other solutes showed no significant differences in mean fluxes between years (NO_3^-, $P = 0.946$; DON, $P = 0.877$; TDN, $P = 0.991$).

Table 1. Soil NO_3^- pools, nitrification rates, and mineralization rates for forest floor and mineral soil horizons measured by three different methods (in situ incubation, laboratory incubation, and laboratory ^{15}N dilution incubation)

Method	NO_3^- pool		Nitrification rates		Mineralization rates	
	Forest floor	Mineral soil	Forest floor	Mineral soil	Forest floor	Mineral soil
	g N m^{-2}		g N m^{-2} day^{-1}		g N m^{-2} day^{-1}	
In situ incubation (net rates)	0.09 (0.01)^{a,A}	0.24 (0.01)^{a,B}	0.01 (0.00)^{a,A,*}	0.01 (0.00)^{a,A,*}	0.04 (0.00)^{a,A,*}	0.03 (0.00)^{a,B,*}
Laboratory incubation (net rates)			0.02 (0.00)^{b,A,*}	0.05 (0.00)^{b,B,*}	0.12 (0.01)^{b,A,*}	0.09 (0.00)^{b,B,*}
Laboratory ^{15}N dilution incubation (gross rates)	0.11 (0.01)^{b,A}	0.22 (0.01)^{a,B}	0.06 (0.01)^{c,A,*}	0.06 (0.01)^{b,A,*}	0.14 (0.01)^{b,A,*}	0.11 (0.01)^{b,A,*}

Sample date and icing treatment were not significant factors ($P > 0.05$), so N variables were averaged across time and treatment for each method. Values are means ($n = 240$ for in situ and laboratory incubation soil NO_3^- pools, which utilized the same set of samples; $n = 280$ for laboratory ^{15}N dilution incubation soil NO_3^- pools; $n = 180$ for in situ incubation rates; $n = 240$ for laboratory incubation rates; and $n = 135$ for laboratory ^{15}N dilution incubation rates) and one standard error (in parentheses). Significance level is $P < 0.05$. For each variable and soil horizon, values with different superscript lowercase letters differ significantly across methods. For each variable and method, values with different superscript uppercase letters differ significantly between the two soil horizons. For each horizon and method, values with superscript asterisks (*) differ significantly between nitrification and mineralization rates.

Table 2. Soil water fluxes of NO_3^-, NH_4^+, DON, and TDN leaching from the B horizon during 2016 and 2017

Treatment	NO_3^-		NH_4^+		DON		TDN	
	g N m^{-2}		g N m^{-2}		g N m^{-2}		g N m^{-2}	
	2016	2017	2016	2017	2016	2017	2016	2017
Control	0.03 (0.01)	0.01 (0.01)	0.00 (0.00)	0.01 (0.00)	0.15 (0.04)	0.16 (0.04)	0.19 (0.04)	0.18 (0.04)
Low	0.02 (0.01)	0.02 (0.01)	0.00 (0.00)	0.01 (0.00)	0.20 (0.05)	0.29 (0.07)	0.22 (0.04)	0.31 (0.06)
Mid	0.01 (0.01)	0.03 (0.01)	0.01 (0.00)	0.01 (0.00)	0.12 (0.03)	0.14 (0.03)	0.13 (0.03)	0.18 (0.04)
Mid × 2	0.02 (0.01)	0.01 (0.01)	0.00 (0.00)	0.01 (0.00)	0.16 (0.04)	0.22 (0.05)	0.18 (0.04)	0.25 (0.05)
High	0.01 (0.01)	0.03 (0.02)	0.00 (0.00)	0.01 (0.00)	0.12 (0.03)	0.18 (0.04)	0.14 (0.03)	0.23 (0.05)

Values are the mean annual sum (g N m^{-2}) and one standard error (in parentheses).

Soil Inorganic N

Soil NO_3^- pools across all ice storm treatments and sampling times were not significantly different and averaged 0.1 g N m^{-2} for the O horizon forest floor and 0.2 g N m^{-2} for the mineral soil (0–15 cm) (Table 1). These pools were significantly different between the two soil horizons (Figure 2), regardless of the analytical method (with the same samples analyzed for both in situ and laboratory incubation methods). Although the NO_3^- pools did not differ between the net rate and gross rate N methods for the mineral soil, the initial concentrations for the samples used in the laboratory ^{15}N dilution incubation were significantly higher (slightly) than those used for the net N cycling rate assays for the forest floor soils.

Net potential nitrification rates (0.01–0.05 g N m^{-2} day^{-1}) for the forest floor and mineral soil were significantly lower than net potential N mineralization rates (0.03–0.12 g N m^{-2} day^{-1}) for each respective soil horizon, for both in situ and laboratory incubation methods (Table 1) when averaged across all ice treatment plots and sampling times. When comparing rates between the two soil horizons, net potential N mineralization rates were significantly higher in the forest floor for both net rate methods, while the mineral soil had significantly higher net potential nitrification rates only when the laboratory incubation method was utilized.

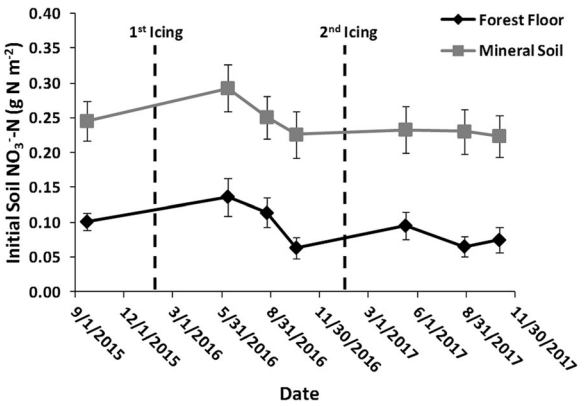

Figure 2. Soil NO_3^- pools in forest floor and mineral soil horizons over seven sample dates from September 2015 to November 2017. Values are means of all treatments for each horizon (n = 240), with vertical bars denoting one standard error. Mineral soil horizon NO_3^- pools were significantly ($P < 0.05$) greater than forest floor pools at all sample dates.

Similar to net N cycling rates, gross rates of nitrification for both the forest floor and mineral soil were significantly lower than gross mineralization rates (Table 1). Gross rates were not significantly different from net potential rates determined via the laboratory incubation method within both soil horizons except for forest floor gross nitrification rates, which were significantly higher than the laboratory net rates (Table 1). Rates of net potential nitrification and mineralization measured using the in situ incubation method were significantly lower for both soil horizons when compared to net and gross rates determined in the laboratory.

All four gross N transformation rates of interest (N mineralization, N immobilization, nitrification, and NO_3^- immobilization) were significantly different across time in both the forest floor and mineral soil horizons, but not across treatments (Figure 3). There were only six instances (out of a possible 20; that is, 5 sampling times × 4 gross N transformation rates = 20 total instances when rates could have been different for the two soil horizons) in which the forest floor and mineral soil had significantly different values at a specific sampling time for each of the four gross N transformation rates. To determine the overall temporal patterns in gross rates, values were combined for all treatments at all sample times for both soil hori-

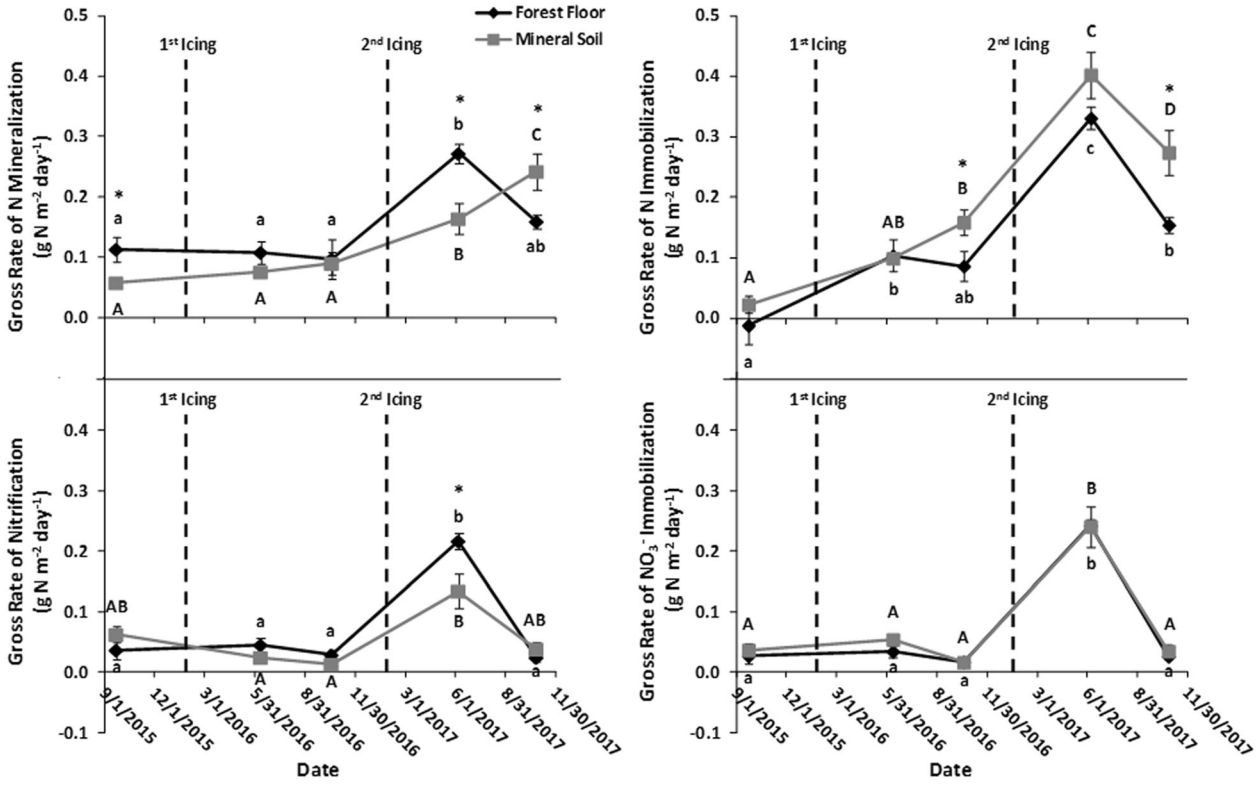

Figure 3. Gross N transformation rates in forest floor and mineral soil horizons over seven sample dates from September 2015 to November 2017. Values are means of all treatments for each horizon (n = 30 for fall 2015; n = 10 for other times), with vertical bars denoting one standard error. Significance level is $P < 0.05$. Values with different lowercase letters differ significantly across time in the forest floor, while values with different uppercase letters differ significantly across time in the mineral soil. Asterisks indicate statistically significant differences between the forest floor and mineral soil.

zons. Results revealed that the overall averages of gross N mineralization (0.12 g N m^{-2} day^{-1}) and gross N immobilization (0.13 g N m^{-2} day^{-1}) rates were not significantly different from one another. These rates were significantly higher than the overall averages of gross nitrification (0.06 g N m^{-2} day^{-1}) and gross NO_3^- immobilization (0.06 g N m^{-2} day^{-1}), which were not significantly different from one another.

Gas Fluxes

Surface fluxes of N_2O from static gas sampling chambers were not significantly different among the different icing treatments or sampling times and averaged 0.14 mg N m^{-2} day^{-1} over the five sampling times (two pre-treatment and three post-treatment dates) (Figure 4). The average post-treatment N_2O surface fluxes were slightly lower (0.07 mg N m^{-2} day^{-1}) than the overall average.

Post-treatment in situ N_2O fluxes across all plots and four sampling times determined from 12 cm intact cores using the N-FARM averaged 1.60 mg m^{-2} day^{-1}, a significantly higher rate than

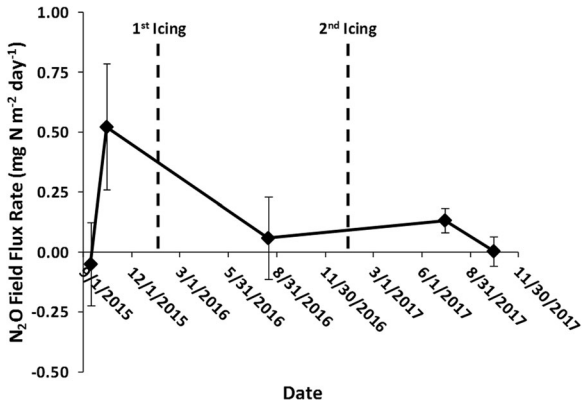

Figure 4. Soil to atmosphere fluxes of N_2O measured from static gas sampling chambers at five sample dates from September 2015 to November 2017. Values are means of all treatment plots for each sampling time (n = 40), with vertical bars denoting one standard error. Neither sample date nor icing treatment was statistically significant ($P < 0.05$).

the fluxes measured in the field chambers. Although the icing treatments did not have statistically significant effects on N_2O fluxes from the

intact cores, fluxes were significantly higher during spring 2017 than on other dates (Figure 5). Fluxes of N_2 measured via the N-FARM were highly variable, spanning orders of magnitude, with no significant differences among icing treatments or sampling times (Figure 6), and an average post-treatment flux of 54.2 mg N m^{-2} day^{-1}. In situ denitrification rates measured via the N-FARM (that is, net production of in situ $N_2O + N_2$) across all ice storm treatment plots and sampling times were not significantly different and averaged 55.8 mg N m^{-2} day^{-1}. Fluxes of N_2 were greater than N_2O (Figures 5 and 6), with an average N_2O yield of 2.9% across all icing treatments and sampling times.

Potential denitrification rates determined via the laboratory-based DEA method were significantly higher than those measured using the N-FARM, averaging 203 mg N m^{-2} day^{-1} for the forest floor horizon and 263 mg N m^{-2} day^{-1} for the mineral soil (Figure 7). These potential denitrification rates were not significantly different among icing treatments, but for both soil horizons, sampling time was statistically significant (Figure 7). Unlike initial NO_3^- pools, potential denitrification rates were not significantly different between the forest floor and mineral soil horizons.

Laboratory incubations of paired N-FARM cores that were a mix of forest floor and mineral soil horizons revealed a significant treatment effect for both initial NO_3^- pools and potential net nitrification rates (significantly lower in the ''mid''-icing treatment than in the other treatments), but not for potential net N mineralization rates (Table 3). Time of sampling was not significantly different for any of the N variables measured from the destructively sampled N-FARM cores. The mixed horizon cores also failed to show any significant differences between potential net rates of N mineralization and nitrification for any of the icing treatments.

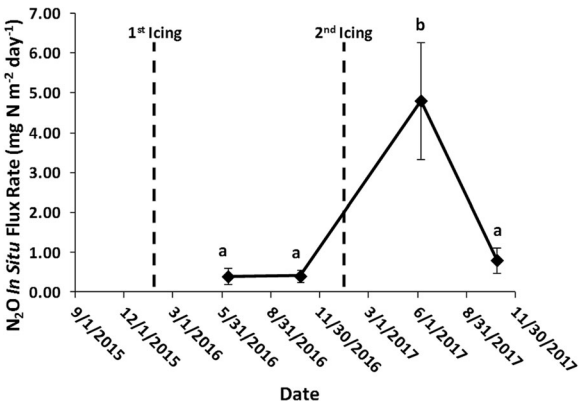

Figure 5. Fluxes of N_2O from intact soil cores measured using the N-free air recirculation method (N-FARM). Values are means of all treatments for each sample date (n = 10), with vertical bars denoting one standard error. Values with different lowercase letters differ significantly ($P < 0.05$) across time. There were no significant differences among icing treatments.

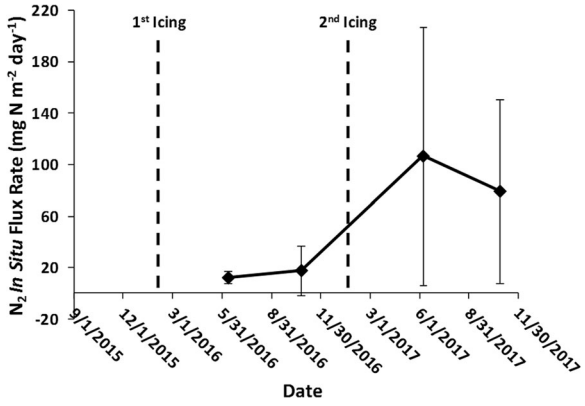

Figure 6. Fluxes of N_2 from intact soil cores measured using the N-free air recirculation method (N-FARM). Values are means of all treatments for each sample date (n = 10), with vertical bars denoting one standard error. Neither sample date nor icing treatment was statistically significant ($P < 0.05$).

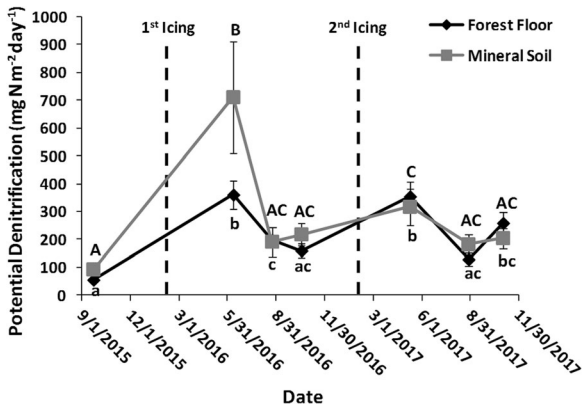

Figure 7. Potential denitrification rates in forest floor and mineral soil horizons over seven sample dates from September 2015 to November 2017. Values are means of all treatments at each sample date (n = 240), with vertical bars denoting one standard error. Significance level is $P < 0.05$. Values with different lowercase letters differ significantly among sampling dates in the forest floor, while values with different uppercase letters differ significantly across dates in the mineral soil. Forest floor and mineral soil horizon potential denitrification rates were not significantly different for any sampling time.

Table 3. Soil NO_3^- pools, nitrification rates, and mineralization rates in intact soil cores used for denitrification measurements (forest floor and mineral soil horizons mixed)

Treatment	Initial NO_3^- pool	Nitrification rates	Mineralization rates
	g N m^{-2}	g N m^{-2} day^{-1}	g N m^{-2}
Control	0.14 (0.04)[a]	0.06 (0.01)[ab]	0.06 (0.01)
Low	0.11 (0.03)[a]	0.08 (0.02)[a]	0.09 (0.01)
Mid	0.02 (0.00)[b]	0.02 (0.01)[b]	0.07 (0.02)
Mid × 2	0.06 (0.01)[ab]	0.03 (0.01)[ab]	0.06 (0.02)
High	0.12 (0.04)[a]	0.05 (0.02)[ab]	0.08 (0.02)

Significance level is $P < 0.05$. Sample date was not a significant factor, so values are means ($n = 8$) and one standard error (in parentheses) for each treatment across all sample dates. Values with different superscript lowercase letters differ significantly across treatments. There were no statistical differences between nitrification and mineralization rates.

Discussion

A Surprising Lack of Response to Icing Treatment

Nitrogen cycle processes showed no response to the imposed ice storm treatments. In contrast to our expectations and observations following a natural ice storm in 1998, we observed no increase in hydrologic losses of N (Table 2) nor changes in soil processes (Table 3), in response to icing amount and frequency. The lack of response in soil processes was less surprising than the lack of response in hydrologic losses, as soil processes also were not responsive to the 1998 storm. Hydrologic losses following the 1998 storm were attributed to reductions in plant uptake due to canopy damage rather than to increases in soil production or decreases in soil consumption of inorganic N (Houlton and others 2003). Thus, we are left with the question whether our experimental ice storm treatments did not decrease plant N uptake as much as the natural 1998 ice storm or perhaps some other factor (for example, N oligotrophication; Groffman and others 2018) underlies the lack of response.

Data on canopy damage collected from the ice storm treatments show that canopy damage was quite severe, though somewhat less intense than for the most severely damaged areas of the HBEF watersheds where soil solution and streamwater NO_3^- increased markedly following the 1998 ice storm (Houlton and others 2003). In particular, measurements of leaf area index (LAI) in the ISE plots indicated that the high icing treatment resulted in about 40% reduction in the first year following treatment, with progressively smaller reductions in the moderate (25%) and low (10%) icing plots (Fahey and others, in revision). Similar measurements in Watershed 1 (W1) in the 1998 ice storm indicated LAI reductions exceeding 50% in the most intensively damaged areas of W1 (Rhoads and others 2002). Moreover, in areas lower in the HBEF watersheds that were less severely damaged in the 1998 ice storm (for example, 20%) no NO_3^- response was observed in soil solutions (Houlton and others 2003); thus, it is possible that the amount of canopy damage in the ISE (at least in the low and moderate treatments) was below a threshold at which soil solution NO_3^- responds.

Notably, the differences among ice intensity treatments were particularly related to vertical reorganization of canopy structure and creation of canopy gaps. There was an overall shift in canopy density to the subcanopy, reflecting both physical displacement of foliage through bending and subcanopy response to the upper canopy disturbance, which matches observational studies of the 1998 ice storm (Beaudet and others 2007; Weeks and others 2009). The subcanopy response could potentially affect total canopy N by promoting growth of vigorous sapling and sprout layer vegetation (Gough and others 2013) as has been observed with recovery from bark beetle outbreaks in western North America (Reed and others 2018). Spring ephemeral plants, which have been invoked as a potential significant N sink at Hubbard Brook (Muller and Bormann 1976), did not visibly respond to the treatment, and represent a small N pool in any case.

We did observe a slight increase in foliar N concentration across all treatments (1.95% in 2015 vs. 2.30% in 2016), and canopy N mass did not decline significantly (RT Fahey, unpublished data), suggesting increased leaf-level N concentrations could have partially mitigated losses in canopy N mass related to leaf area reduction (Nave and others 2011). After the 1998 ice storm, there was no evidence for increased foliar N in the post-storm years, indicating reduced N uptake was proportional to the reduced leaf mass. Thus, N uptake in 1998 was

likely reduced to a greater degree than in the current study, partially explaining the larger N loss in 1998.

Another possible factor contributing to the limited N cycle responses in this ice storm experiment compared with the 1998 ice storm is the scale of the treatments. Whereas in the natural ice storm the damage occurred across very large scales (though highly patchy; Rhoads and others 2003), in this experiment the scale of canopy damage was roughly 600 m^2, the size of the treatment plots. Thus, the experimental ice storm simulated a canopy gap regime rather than a large-scale, diffuse disturbance (Beaudet and others 2007). Although edge effects were likely reduced by the 5 m buffer around the plots, it is possible that root systems of trees from outside the plots played a role in N uptake and retention. Of note, ingrowth core sampling of root growth in the plots detected no treatment effects (TJ Fahey, unpublished data), but whether this resulted from root growth of trees from inside or outside the plots is unclear. Bauhus and Bartsch (1996) noted that roots of trees surrounding 30-m-diameter canopy gaps in *Fagus sylvatica* forest did not extend 10 m to the center of the gaps. The effects of gap size on N cycling processes have been found to be highly variable among forest types and soils (Parsons and others 1994; Denslow and others 1998; McCarthy 2001; Scharenbroch and Bockheim 2007), and the role of this factor in the present study is uncertain. Most important is that our main hydrologic response for comparison between the 1998 and current study was soil solution chemistry/leaching, measured with lysimeters, which are much more appropriate for plot studies. Our other response variables in the soil and soil/atmosphere gas fluxes are also less of a concern in small plot studies.

A key factor in the 1998 study was previous land use. A survey of watersheds in the area surrounding Hubbard Brook found that areas with a history of previous agricultural land use (that likely depleted N through persistent crop removals) did not show a marked N response to the ice storm. The experimental plots for this study do not have a history of agricultural land use, and thus, differences in land use history do not account for the contrast in responses between this study and the 1998 ice storm.

Comparison of soil process data for this experiment with observations from 1998 (Houlton and others 2003), in which the same exact methods were used to measure in situ and laboratory rates, suggests that the ecosystems experiencing the experimental ice storm treatments are cycling N more slowly than the sites affected by the 1998 storm. We measured in situ rates of N mineralization of less than 0.05 g N m^{-2} day^{-1} and in situ rates of nitrification of 0.01 g N m^{-2} day^{-1} (Table 1), whereas mineralization rates in 1998 were greater than 0.20 g N m^{-2} day^{-1} and nitrification rates were greater than 0.15 g N m^{-2} day^{-1}. Most relevant here are annual measurements of potential net N mineralization since 1994 that have declined markedly and significantly since that time (Figure 8A). Fluxes of N_2O from soil to the atmosphere have also declined markedly and significantly over the same period (Figure 8B; Groffman and others 2018).

In addition to declines in N mineralization, other N cycle variables that we measured in the ice storm manipulation plots were low relative to previous studies at the HBEF. Concentrations of soil solution NO_3^- in the B horizon, which has been shown to be highly responsive to various disturbances in previous studies at the HBEF (for example, Fitzhugh and others 2001; Houlton and others 2003), remained relatively low throughout the pre- and post-treatment periods (maximum = 0.22 mg N l^{-1}; mean = 0.01 mg N l^{-1}) and were typically below or near detection limits (0.01 mg N l^{-1}) during the growing season. These NO_3^- values are comparable to concentrations (maximum = 0.24 mg N l^{-1}, mean = 0.02 mg N l^{-1}) measured with tension lysimeters from 2008 to 2010 in control plots of a soil freezing experiment located 500 m from the ISE plots (Campbell and others 2014). However, in that experiment, NO_3^- concentrations increased in response to the freezing disturbance, to a peak concentration of 3.3 mg N l^{-1} during the growing season, whereas there was no NO_3^- response in the 2-year following our ice treatments here. Concentrations of NO_3^- in freely draining soil water in areas affected by the 1998 ice storm (that is, Watershed 1 which is 3.2 km from the ISE plots) in the year prior to the 1998 ice storm were lower (mean = 0.6 mg N l^{-1} in Bs and 0.3 mg N l^{-1} in Bh horizons) than measurements following the 1998 ice storm (Houlton and others 2003). In the year after the natural ice storm, average NO_3^- concentrations increased to 2.1 mg N l^{-1} in the Bs and 1.6 mg N l^{-1} in the Bh horizons. Thus, the soil solution NO_3^- concentrations and disturbance responses that we observed support ideas about the development of N oligotrophication at the HBEF and suggest that this has altered the nature of N cycle responses to disturbance.

In contrast to hydrologic losses, gaseous loss of N in our ice storm manipulation plots was not low

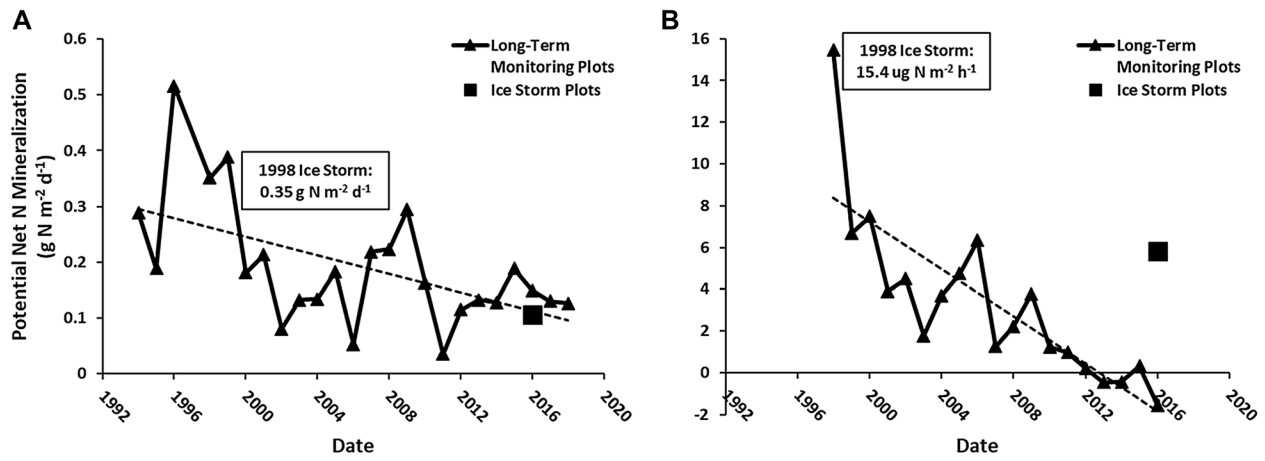

Figure 8. **A** Potential net N mineralization in long-term monitoring and ice storm manipulation plots. Values for the long-term monitoring plots are means of Oie horizon samples from 20 plots along an elevation gradient (five plots per elevation) sampled in mid-summer of each year in a mature reference forest. The value for the ice storm manipulation plots is a mean of all Oie horizon samples across all ice storm plots sampled seven times between September 2015 and November 2017. **B** Soil to atmosphere nitrous oxide fluxes in long-term monitoring and ice storm manipulation plots. Values for the long-term monitoring plots are means of a variable number of sites, sampled at variable frequencies in different years along an elevation gradient in HBEF. The value for the ice storm manipulation plots is the mean nitrous oxide flux measured from static gas sampling chambers across all ice storm plots sampled five times between September 2015 and November 2017.

relative to previous studies at the HBEF (Figure 8B). Fluxes of N_2O measured in 2015–2017 from the static gas chambers in the ISE control plots averaged 18.8 μg N m^{-2} h^{-1}, which are similar to rates measured along elevation gradients at the HBEF after the natural ice storm (15.4 μg N m^{-2} h^{-1}), that have declined markedly since that time (Groffman and others 2018). Mean gaseous fluxes of N_2O and N_2 measured in the ISE control plots in the spring and fall of 2016 and 2017 using the N-FARM (Figures 5 and 6) were higher than fluxes measured in the spring, summer, and fall from November 2010 to August 2012 from other sites at the HBEF (Morse and others 2015a, b). Fluxes of N_2O and N_2 from the ISE control plots averaged 36 μg N m^{-2} h^{-1} and 321 μg N m^{-2} h^{-1}, respectively, whereas N_2O and N_2 fluxes measured in previous years at other HBEF sites averaged 12 μg N m^{-2} h^{-1} and 50 μg N m^{-2} h^{-1}, respectively. The comparison with previous gas fluxes must be interpreted with caution as they are based on limited sampling and at different sites. Still, these results are consistent with the idea that gaseous N fluxes are higher than expected and that hot spots of these fluxes may be contributing to N oligotrophication at the ice storm site.

Potential denitrification rates in the forest floor throughout the HBEF measured in 1994–2014 showed a decreasing long-term trend, and rates in the ISE plots appear to continue this downward trend in 2015–2017, averaging about 740 μg N (kg soil)$^{-1}$ h^{-1}. No clear trends in potential denitrification rates are evident over the same time period for the mineral soil at the HBEF, but measured rates in the ISE plots averaged about 200 μg N (kg soil)$^{-1}$ h^{-1}, which falls within the range of values recorded from 1994 to 2014 (~ 50–400 μg N (kg soil)$^{-1}$ h^{-1}).

Our results are consistent with significant regional changes in N cycling that have been observed in northeastern North America (Groffman and others 2018; Gilliam and others 2019). Both atmospheric deposition (Eshleman and others 2013; Li and others 2016; Lloret and Valiela 2016) and watershed exports of N (Goodale and others 2003; Kothawala and others 2011; Yanai and others 2013; Driscoll and others 2016; Stevens 2016) have declined across the region. This N ''oligotrophication'' has, under certain circumstances, like soil freezing, altered what was once the typical response of the ecosystem N cycle to disturbance (Judd and others 2011; Fuss and others 2016b).

At Hubbard Brook, mass-balance analyses show that both inputs and outputs of N have both greatly decreased over recent decades. At its peak in the 1960s–1970s, total atmospheric N inputs averaged 9.5 kg N ha^{-1} y^{-1}, but have since declined to less than 6 kg N ha^{-1} y^{-1} (Yanai and others 2013). Biological N_2 fixation was measured in decaying wood in the late 1970s (Roskowski 1980) at less than 2 kg N ha^{-1} y^{-1}, whereas the natural background rates of fixation are likely below 1 kg N ha^{-}

^{1} y^{-1}. Of the total atmospheric inputs to HBEF, about 6% has been attributed to dry deposition of particulate and gaseous N (Yanai and others 2013). Outputs of N in the 1960s–1970s in streamwater averaged 4.5 kg N ha^{-1} y^{-1} (Yanai and others 2013)—close to the combined inputs from N_2 fixation and background atmospheric deposition. However, N in streamwater declined rapidly in the late 1970s and has averaged less than 1.5 kg N ha^{-1} y^{-1} for the past 30+ years (Yanai and others 2013), which is much lower than inputs. Gaseous losses of N may contribute an important missing sink for this imbalance between N inputs and outputs at HBEF (Groffman and others 2009; Morse and others 2015b), as could storage in the soil N pool which could be ''mined'' or ''replenished'' depending on forest N requirements (Lovett and others 2018).

N Oligotrophication and Response to Disturbance

There is a long history of research in ecology suggesting that the potential for hydrologic losses of N following disturbance can be predicted by rates of net N mineralization and nitrification (Vitousek and others 1979), such that sites with high rates of N mineralization lose more N following disturbance than sites with low mineralization rates. Our results are consistent with this paradigm, where decreases in N mineralization and nitrification since 1998 appear to have made the ecosystems at the HBEF less susceptible to drainage NO_3^- losses from our experimental ice storm disturbances.

We also measured gross rates of N cycle processes in the experimental icing treatments (Figure 3), which were not measured in 1998, with the idea that this metric might be more responsive to the ice storm disturbance than the net rates. However, gross rates did not respond to the treatment any more than net rates. Though measured at different sites and only in the forest floor, gross rates measured in 1999 and 2000 (Groffman and others 2006) were similar to the rates measured here, suggesting (weakly) that N oligotrophication at the HBEF may not be driven by changes in gross rates of N cycle processes.

There is a clear need for further research into the drivers of the ongoing N oligotrophication that has been observed at the HBEF and some other forest sites in eastern North America (Groffman and others 2018; Gilliam and others 2019). Although the region has experienced significant declines in atmospheric deposition of N in recent decades (Lloret and Valiela 2016), declines in streamwater export and soil cycling of N do not always coincide with these declines (Sabo and others 2016), suggesting other drivers, such as changes in climate (Durán and others 2016), elevated atmospheric CO_2 (Mathias and Thomas 2018), or deacidification (Oulehle and others 2011) may play a role. Further analysis of gross soil N cycling rates, which are closely coupled to C cycling (Hart and others 1994b), might shed light on the idea that changes in the C cycle are an important driver of N oligotrophication in these forests. One hypothesis is that additional C flow from the atmosphere and/or resulting from deacidification has driven significant amounts of N from the active cycling pool into more stable forms of organic matter (Cotrufo and others 2013). In concert with declining inputs of N from the atmosphere, these changes may have reduced the size of the active N cycling pool that is a proximal source of plant-available and readily mobilized N following disturbance. An additional hypothesis is that increases in plant uptake, possibly driven by a longer growing season, reduce the size of the active N cycling pool in soil (Keenan and others 2014).

Links between C and N cycling are particularly interesting in the context of ice storms, which create a pulse of fine and coarse litter input to the soil. Surprisingly, soil solution NO_3^- following the ice storm of 1998 remained low throughout the growing season even though the vegetation was severely damaged and NO_3^- production (that is, nitrification) is typically highest during that time of year (Houlton and others 2003). Peak soil solution NO_3^- concentrations in the B horizon that resulted from the 1998 ice storm occurred during the fall (September and November) after the disturbance and remained elevated for a year. This delayed NO_3^- response to the natural ice storm was attributed to enhanced immobilization of N by soil microbiota as a result of the influx of fine and coarse litter with high C/N ratios (Houlton and others 2003). Although results from the ice storm experiment show no comparable increase in soil solution NO_3^- after 2 years (Table 2), N immobilization associated with enhanced litter inputs may have contributed to the lack of response.

Similar to the ice storm responses reported here, changes in the C cycle have affected ecosystem N cycling response to soil freezing disturbance at the HBEF. Responses to a series of experimentally induced and natural soil freezing events that have occurred since the late 1990s have shown the same declining sensitivity to disturbance that we observed for ice storms (Judd and others 2011; Fuss

and others 2016a, b). In contrast to our ice storm manipulation, which does not appear to mobilize labile C over the short term, soil freezing appears to mobilize dissolved organic C (DOC) which can directly prevent or mask an N response by stimulating N immobilization and/or denitrification (Groffman and others 2010; Fuss and others 2016a). This mobilization of DOC, which is likely driven by physical disruption of primary and secondary soil particles and roots by soil freezing (Cleavitt and others 2008), was much more marked in freezing disturbance studies in 2003/2004 and 2011/2012 than in earlier studies in 1997/1998. These results suggest that changes in the C cycle can affect ecosystem N cycle response both by driving declines in the active N cycling pool and by creating a pool of DOC that is readily mobilized following disturbance.

Implications for Resilience

Our results have implications for assessment of the response of ecosystem N cycling to and recovery from a wide range of disturbances. Changes in ecosystem response to ice storm and soil freezing disturbance over the past 20 years, perhaps driven by N oligotrophication, suggest that while the water quality and greenhouse gas impacts of these disturbances have decreased, the ability of the ecosystem to recover from these disturbances may be reduced or delayed, compared to conditions under which N was readily accessible to support rapid plant regrowth. The 1998 ice storm and soil freezing manipulations in the late 1990s produced marked increases in hydrologic N losses, with concentrations in streamwater similar to those seen following clear cutting at the HBEF (Dahlgren and Driscoll 1994). The ice storm manipulations here, and both natural and induced soil freezing events from 2003 to 2012, have not increased N concentrations in streams or watershed N exports. These changes are likely to improve ecosystem services, as mitigation of N losses should enhance the fertility of forest ecosystems and production of biomass, while limiting the eutrophication of receiving waters (Beier and others 2015; Caputo and others 2016a, b). However, the mobilization of reactive N by disturbance facilitates rapid regrowth of vegetation and re-establishment of biotic control over the abiotic environment, a fundamental component of recovery (Bormann and Likens 1979). Recovery from the 1998 ice storm was rapid, with prompt canopy regrowth facilitating re-establishment of leaf area and a return to baseline watershed N exports within 3 years (Houlton and others 2003). Continued monitoring of the ISE plots is needed to determine whether recovery on our ice storm manipulation plots will extend longer than 3 years and if this delay leads to other changes in the ecosystem (for example, colonization by new species taking advantage of a more open canopy, delayed wound closure on damaged trees).

Conceptually, the hypothesis that N cycling is tightening over time greatly complicates assessment of disturbance, recovery, and resilience. If baseline N cycling processes are decreasing over time, predictions of the effects of disturbance, and evaluation of the nature and extent of recovery become much more complex. Mechanistic uncertainty about changes in baseline processes further increases uncertainty. Moreover, the possible contribution of disturbance scale in affecting the differential response to natural and experimental ice storms only increases the level of uncertainty. Assessments of disturbance, recovery, and resilience are already great challenges in ecosystem science, and complex alterations in ecosystem processes driven by multiple components of environmental change substantially increase these challenges.

ACKNOWLEDGEMENTS

Funding for this research was provided by the National Science Foundation (DEB-1457675). We thank all the people who helped with the ice application and associated field and laboratory work, especially Ian Halm, Frank Bowles, Geoff Schwaner, Gabe Winant, and Brendan Leonardi. This manuscript is a contribution of the Hubbard Brook Ecosystem Study. Hubbard Brook is part of the Long-Term Ecological Research (LTER) network, which is supported by the National Science Foundation (DEB-1633026). The Hubbard Brook Experimental Forest (HBEF) is operated and maintained by the USDA Forest Service, Northern Research Station, Newtown Square, PA.

DATA AVAILABILITY

The data for this paper are available through the Hubbard Brook Data Catalog (https://hubbardbrook.org/d/hubbard-brook-data-catalog).

Compliance with Ethical Standards

Conflict of interest The authors declare that they have no conflict of interest.

REFERENCES

Bauhus J, Bartsch N. 1996. Fine-root growth in beech (*Fagus sylvatica*) forest gaps. Can J For Res 26:2153–9.

Beaudet M, Brisson J, Messier C, Gravel D. 2007. Effect of a major ice storm on understory light conditions in an old-growth Acer-Fagus forest: pattern of recovery over seven years. For Ecol Manage 242:553–7.

Beier CM, Caputo J, Groffman PM. 2015. Measuring ecosystem capacity to provide regulating services: forest removal and recovery at Hubbard Brook (USA). Ecol Appl 25:2011–21.

Binkley D, Hart SC. 1989. The components of nitrogen availability assessments in forest soils. Adv Soil Sci 10:57–112.

Bormann FH, Likens GE. 1979. Pattern and process in a forested ecosystem. New York: Springer-Verlag New York. p 272p.

Bowden RD, Melillo JM, Steudler PA, Aber JD. 1991. Effects of nitrogen additions on annual nitrous-oxide fluxes from temperate forest soils in the northeastern United States. J Geophys Res Atmos 96:9321–8.

Burgin AJ, Groffman PM. 2012. Soil O_2 controls denitrification rates and N_2O yield in a riparian wetland. J Geophys Res Biogeosci 117:G01010.

Burgin AJ, Groffman PM, Lewis DN. 2010. Factors regulating denitrification in a riparian wetland. Soil Sci Soc Am J 74:1826–33.

Campbell JL, Socci AM, Templer PH. 2014. Increased nitrogen leaching following soil freezing is due to decreased root uptake in a northern hardwood forest. Glob Change Biol 20:2663–73.

Caputo J, Beier CM, Groffman PM, Burns DA, Beall FD, Hazlett PW, Yorks TE. 2016a. Effects of harvesting forest biomass on water and climate regulation services: A synthesis of long-term ecosystem experiments in eastern North America. Ecosystems 19:271–83.

Caputo J, Beier CM, Luzadis VA, Groffman PM. 2016b. Integrating beneficiaries into assessment of ecosystem services from managed forests at the Hubbard Brook Experimental Forest, USA. For Ecosyst 3:13.

Changnon S. 2003. Characteristics of ice storms in the United States. J Appl Meteorol 42:630–9.

Cheng CS, Auld H, Li G, Klaasen J, Li Q. 2007. Possible impacts of climate change on freezing rain in south-central Canada using downscaled future climate scenarios. Nat Hazards Earth Syst Sci 7:71–87.

Cheng CS, Li G, Auld H. 2011. Possible impacts of climate change on freezing rain using downscaled future climate scenarios: updated for eastern Canada. Atmos Ocean 49:8–21.

Christenson LM, Lovett GM, Weathers KC, Arthur MA. 2009. The influence of tree species, nitrogen fertilization, and soil C to N ratio on gross soil nitrogen transformations. Soil Sci Soc Am J 73:638–46.

Cleavitt NL, Fahey TJ, Groffman PM, Hardy JP, Henry KS, Driscoll CT. 2008. Effects of soil freezing on fine roots in a northern hardwood forest. Can J For Res 38:82–91.

Cotrufo MF, Wallenstein MD, Boot CM, Denef K, Paul E. 2013. The Microbial Efficiency-Matrix Stabilization (MEMS) framework integrates plant litter decomposition with soil organic matter stabilization: do labile plant inputs form stable soil organic matter? Glob Change Biol 19:988–95.

Dahlgren RA, Driscoll CT. 1994. The effects of whole-tree clear-cutting on soil processes at the Hubbard Brook Experimental Forest, New Hampshire, USA. Plant Soil 158:239–62.

Davidson EA, Hart SC, Shanks CA, Firestone MK. 1991. Measuring gross nitrogen mineralization, and nitrification by 15N isotopic pool dilution in intact soil cores. Eur J Soil Sci 42:335–49.

Denslow JS, Ellison AM, Sanford RE. 1998. Treefall gap size effects on above- and below-ground processes in a tropical wet forest. J Ecol 86:597–609.

Driscoll CT, Driscoll KM, Fakhraei H, Civerolo K. 2016. Long-term temporal trends and spatial patterns in the acid-base chemistry of lakes in the Adirondack region of New York in response to decreases in acidic deposition. Atmos Environ 146:5–14.

Durán J, Morse JL, Groffman PM. 2012. Comparison of in situ methods to measure N mineralization rates in forest soils. Soil Biol Biochem 46:145–7.

Durán J, Morse JL, Groffman PM, Campbell JL, Christenson LM, Driscoll CT, Fahey TJ, Fisk MC, Likens GE, Melillo JM, Mitchell MJ, Templer PH, Vadeboncoeur MA. 2016. Climate change decreases nitrogen pools and mineralization rates in northern hardwood forests. Ecosphere 7:e01251.

Eshleman KN, Sabo RD, Kline KM. 2013. Surface water quality is improving due to declining atmospheric N deposition. Environ Sci Technol 47:12193–200.

Fahey TJ, Siccama TG, Driscoll CT, Likens GE, Campbell J, Johnson CE, Battles JJ, Aber JD, Cole JJ, Fisk MC, Groffman PM, Hamburg SP, Holmes RT, Schwarz PA, Yanai RD. 2005. The biogeochemistry of carbon at Hubbard Brook. Biogeochemistry 75:109–76.

Federer CA. 2017. BROOK 90: a simulation model for evaporation, soil water, and streamflow. http://www.ecoshift.net/brook/brook90.htm.

Federer CA, Turcotte DE, Smith CT. 1993. The organic fraction—bulk density relationship and the expression of nutrient content in forest soils. Can J For Res 23:1026–32.

Fitzhugh RD, Driscoll CT, Groffman PM, Tierney GL, Fahey TJ, Hardy JP. 2001. Effects of soil freezing disturbance on soil solution nitrogen, phosphorus, and carbon chemistry in a northern hardwood ecosystem. Biogeochemistry 56:215–38.

Fuss CB, Driscoll CT, Green MB, Groffman PM. 2016a. Hydrologic flowpaths during snowmelt in forested headwater catchments under differing winter climatic and soil frost regimes. Hydrol Process 30:4617–32.

Fuss CB, Driscoll CT, Groffman PM, Campbell JL, Christenson LM, Fahey TJ, Fisk MC, Mitchell MJ, Templer PH, Durán J, Morse JL. 2016b. Nitrate and dissolved organic carbon mobilization in response to soil freezing variability. Biogeochemistry 131:35–47.

Galloway JN, Aber JD, Erisman JW, Seitzinger SP, Howarth RW, Cowling EB, Cosby BJ. 2003. The nitrogen cascade. Bioscience 53:341–56.

Gilliam FS, Burns DA, Driscoll CT, Frey SD, Lovett GM, Watmough SA. 2019. Decreased atmospheric nitrogen deposition in eastern North America: predicted responses of forest ecosystems. Environ Pollut 244:560–74.

Goodale CL, Aber JD, Vitousek PM. 2003. An unexpected nitrate decline in New Hampshire streams. Ecosystems 6:75–86.

Gough CM, Hardiman BS, Nave LE, Bohrer G, Maurer KD, Vogel CS, Nadelhoffer KJ, Curtis PS. 2013. Sustained carbon uptake and storage following moderate disturbance in a Great Lakes forest. Ecol Appl 23:1202–15.

Grimm NB, Staudinger MD, Staudt A, Carter SL, Chapin FS, Kareiva P, Ruckelshaus M, Stein BA. 2013. Climate-change

impacts on ecological systems: introduction to a US assessment. Front Ecol Environ 11:456–64.

Groffman PM, Holland EA, Myrold DD, Robertson GP, Zou X. 1999. Denitrification. In: Robertson GP, Bledsoe CS, Coleman DC, Sollins P, Eds. Standard soil methods for long term ecological research. New York: Oxford University Press. p 272–88.

Groffman PM, Fisk MC, Driscoll CT, Likens GE, Fahey TJ, Eagar C, Pardo LH. 2006. Calcium additions and microbial nitrogen cycle processes in a northern hardwood forest. Ecosystems 9:1289–305.

Groffman PM, Hardy JP, Fisk MC, Fahey TJ, Driscoll CT. 2009. Climate variation and soil carbon and nitrogen cycling processes in a northern hardwood forest. Ecosystems 12:927–43.

Groffman PM, Hardy JP, Fashu-Kanu S, Driscoll CT, Cleavitt NL, Fahey TJ, Fisk MC. 2010. Snow depth, soil freezing and nitrogen cycling in a northern hardwood forest landscape. Biogeochemistry 102:223–38.

Groffman PM, Driscoll CT, Durán J, Campbell JL, Christenson LM, Fahey TJ, Fisk MC, Fuss C, Likens GE, Lovett G, Rustad L, Templer PH. 2018. Nitrogen oligotrophication in northern hardwood forests. Biogeochemistry 141:123–9.

Gyakum JR, Roebber PJ. 2001. The 1998 ice storm-analysis of a planetary-scale event. Mon Weather Rev 129:2983–97.

Hart SC, Stark JM. 1997. Nitrogen limitation of the microbial biomass in old-growth forest soil. Ecoscience 4:91–8.

Hart SC, Nason GE, Myrold DD, Perry DA. 1994a. Dynamics of gross nitrogen transformations in an old-growth forest: the carbon connection. Ecology 75:880–91.

Hart SC, Stark JM, Davidson EA, Firestone MK. 1994b. Nitrogen mineralization, immobilization, and nitrification. In: Bottomley PS, Angle JS, Weaver RW, Eds. Methods of soil analysis, part 2, microbiological and biochemical properties. Madison: Soil Science Society of America. p 985–1018.

Hayhoe K, Wake CP, Huntington TG, Luo LF, Schwartz MD, Sheffield J, Wood E, Anderson B, Bradbury J, DeGaetano A, Troy TJ, Wolfe D. 2007. Past and future changes in climate and hydrological indicators in the US Northeast. Clim Dyn 28:381–407.

Houlton BZ, Driscoll CT, Fahey TJ, Likens GE, Groffman PM, Bernhardt ES, Buso DC. 2003. Nitrogen dynamics in ice storm-damaged forest ecosystems: implications for nitrogen limitation theory. Ecosystems 6:431–43.

Judd K, Likens G, Buso D, Bailey A. 2011. Minimal response in watershed nitrate export to severe soil frost raises questions about nutrient dynamics in the Hubbard Brook experimental forest. Biogeochemistry 106:443–59.

Keenan TF, Gray J, Friedl MA, Toomey M, Bohrer G, Hollinger DY, Munger JW, O'Keefe J, Schmid HP, Wing IS, Yang B, Richardson AD. 2014. Net carbon uptake has increased through warming-induced changes in temperate forest phenology. Nat Clim Change 4:598–604.

Kirkham D, Bartholomew WV. 1954. Equation for following nutrient transformations in soil utilizing tracer data. Soil Sci Soc Am Proc 18:33–4.

Knoepp JD, Swank WT. 1995. Comparison of available soil nitrogen assays in control and burned forested sites. Soil Sci Soc Am J 59:1750–4.

Kothawala DN, Watmough SA, Futter MN, Zhang L, Dillon PJ. 2011. Stream nitrate responds rapidly to decreasing nitrate deposition. Ecosystems 14:274–86.

Kranabetter JM, McLauchlan KK, Enders SK, Fraterrigo JM, Higuera PE, Morris JL, Rastetter EB, Barnes R, Buma B, Gavin DG, Gerhart LM, Gillson L, Hietz P, Mack MC, McNeil B, Perakis S. 2016. A framework to assess biogeochemical response to ecosystem disturbance using nutrient partitioning ratios. Ecosystems 19:387–95.

Lafon CW. 2004. Ice-storm disturbance and long-term forest dynamics in the Adirondack Mountains. J Veg Sci 15:267–76.

Li Y, Schichtel BA, Walker JT, Schwede DB, Chen X, Lehmann CMB, Puchalski MA, Gay DA, Collett JA. 2016. Increasing importance of deposition of reduced nitrogen in the United States. Proc Natl Acad Sci USA 113:5874–9.

Likens GE. 2013. Biogeochemistry of a forested ecosystem. 3rd edn. New York: Springer-Verlag New York. p 208p.

Lloret J, Valiela I. 2016. Unprecedented decrease in deposition of nitrogen oxides over North America: the relative effects of emission controls and prevailing air-mass trajectories. Biogeochemistry 129:165–80.

Lovett GM, Goodale CL, Ollinger SV, Fuss CB, Ouimette AP, Likens GE. 2018. Nutrient retention during ecosystem succession: a revised conceptual model. Front Ecol Environ 16:532–8.

Mathias JM, Thomas RB. 2018. Disentangling the effects of acidic air pollution, atmospheric CO_2, and climate change on recent growth of red spruce trees in the Central Appalachian Mountains. Glob Change Biol 24:3938–53.

Matson PA, Vitousek PM. 1981. Nitrogen mineralization and nitrification potentials following clearcutting in the Hoosier national forest, Indiana. For Sci 27:781–91.

McCarthy J. 2001. Gap dynamics of forest trees: a review with particular attention to boreal forests. Environ Rev 9:1–59.

Miller-Weeks M, Eagar C, Petersen CM. 1999. The northeastern ice storm 1998, a forest damage assessment for New York. Vermont, New Hampshire, and Maine: North East State Foresters Association. p 32p.

Morse JL, Durán J, Beall F, Enanga E, Creed IF, Fernandez IJ, Groffman PM. 2015a. Soil denitrification fluxes from three northeastern North American forests across a range of nitrogen deposition. Oecologia 177:17–27.

Morse JL, Durán J, Groffman PM. 2015b. Denitrification and greenhouse gas fluxes in a northern hardwood forest: the importance of snowmelt and implications for ecosystem N budgets. Ecosystems 18:520–32.

Muller RN, Bormann FH. 1976. Role of *Erythronium americanum* Ker. in energy flow and nutrient dynamics of a northern hardwood forest ecosystem. Science 193:1126–8.

Nave LE, Gough CM, Maurer KD, Bohrer G, Hardiman BS, Le Moine J, Munoz AB, Nadelhoffer KJ, Sparks JP, Strahm BD, Vogel CS. 2011. Disturbance and the resilience of coupled carbon and nitrogen cycling in a north temperate forest. J Geophys Res Biogeosci 116:G04016.

Nelson DW, Sommers LE. 1996. Total carbon, organic carbon, and organic matter. In: Sparks DL, Page AL, Helmke PA, Loeppert RH, Soltanpour PN, Tabatabai MA, Johnston CT, Sumner ME, Eds. Methods of soil analysis, part 3, chemical methods. Madison: Soil Science Society of America. p 1001–5.

Niu S, Classen AT, Dukes JS, Kardol P, Liu L, Luo Y, Rustad L, Sun J, Tang J, Templer PH, Thomas RQ, Tian D, Vicca S, Wang YP, Xia J, Zaehle S. 2016. Global patterns and substrate-based mechanisms of the terrestrial nitrogen cycle. Ecol Lett 19:697–709.

Oulehle F, Evans CD, Hofmeister J, Krejci R, Tahovska K, Persson T, Cudlin P, Hruska J. 2011. Major changes in forest

carbon and nitrogen cycling caused by declining sulphur deposition. Glob Change Biol 17:3115–29.

Parsons WFJ, Knight DH, Miller SL. 1994. Root gap dynamics in lodgepole pine forest: nitrogen transformations in gaps of different size. Ecol Appl 4:354–62.

Peters DPC, Lugo AE, Chapin FS, Pickett STA, Duniway M, Rocha AV, Swanson FJ, Laney C, Jones J. 2011. Cross-system comparisons elucidate disturbance complexities and generalities. Ecosphere 2:art81.

Pickett STA, White PS. 1983. The ecology of natural disturbance and patch dynamics. New York: Academic Press. p 472p.

Ratajczak Z, Carpenter SR, Ives AR, Kucharik CJ, Ramiadantsoa T, Stegner MA, Williams JW, Zhang J, Turner MG. 2018. Abrupt change in ecological systems: inference and diagnosis. Trends Ecol Evol 33:513–26.

Reed DE, Ewers BE, Pendall E, Frank J, Kelly R. 2018. Bard beetle-induced tree mortality alters stand energy budgets due to water budget changes. Theor Appl Climatol 131:153–65.

Rhoads AG, Hamburg SP, Fahey TJ, Siccama TG, Hane EN, Battles J, Cogbill C, Randall J, Wilson G. 2002. Effects of an intense ice storm on the structure of a northern hardwood forest. Can J For Res 32:1763–75.

Robertson GP, Wedin D, Groffman PM, Blair JM, Holland EA, Nadelhoffer KA, Harris D. 1999. Soil carbon and nitrogen availability: nitrogen mineralization, nitrification and carbon turnover. In: Robertson GP, Bledsoe CS, Coleman DC, Sollins P, Eds. Standard soil methods for long term ecological research. New York: Oxford University Press. p 258–71.

Roskowski J. 1980. Nitrogen fixation in hardwood forests of the northeastern United States. Plant Soil 54:33–44.

Rustad LE, Campbell JL. 2012. A novel ice storm manipulation experiment in a northern hardwood forest. Can J For Res 42:1810–18.

Sabo RD, Scanga SE, Lawrence GB, Nelson GM, Eshleman KN, Zabala GA, Alinea AA, Schirmer CD. 2016. Watershed-scale changes in terrestrial nitrogen cycling during a period of decreased atmospheric nitrate and sulfur deposition. Atmos Environ 146:271–9.

Salonen K. 1979. The selection of temperature for high temperature combustion of carbon. Acta Hydrochim Hydrobiol 7:591–7.

Santisteban JI, Mediavilla R, López-Pamo E, Dabrio CJ, Zapata MBR, García MJG, Castaño S, Martínez-Alfaro PE. 2004. Loss on ignition: a qualitative or quantitative method for organic matter and carbonate mineral content in sediments? J Paleolimnol 32:287–99.

Scharenbroch BC, Bockheim JG. 2007. Impacts of forest gaps on soil properties and processes in old growth northern hardwood-hemlock forests. Plant Soil 294:219–33.

Smith MS, Tiedje JM. 1979. Phases of denitrification following oxygen depletion in soil. Soil Biol Biochem 11:262–7.

Stark JM, Hart SC. 1996. Diffusion technique for preparing salt solutions, Kjeldahl digests, and persulfate digests for nitrogen-15 analysis. Soil Sci Soc Am J 60:1846–55.

Stevens CJ. 2016. How long do ecosystems take to recover from atmospheric nitrogen deposition? Biol Conserv 200:160–7.

Turner MG. 2010. Disturbance and landscape dynamics in a changing world. Ecology 91:2833–49.

Venterea RT, Groffman PM, Verchot LV, Magill AH, Aber JD. 2004. Gross nitrogen process rates in temperate forest soils exhibiting symptoms of nitrogen saturation. For Ecol Manage 196:129–42.

Vitousek PM, Gosz JR, Grier CC, Melillo JM, Reiners WA, Todd RL. 1979. Nitrate losses from disturbed ecosystems. Science 204:469–74.

Vitousek PM, Gosz JR, Grier CC, Melillo JM, Reiners WA. 1982. A comparative analysis of potential nitrification and nitrate mobility in forest ecosystems. Ecol Monogr 52:155–77.

Weeks BC, Hamburg SP, Vadeboncoeur MA. 2009. Ice storm effects on the canopy structure of a northern hardwood forest after eight years. Can J For Res 39:1475–83.

Wuebbles D, Meehl G, Hayhoe K, Karl TR, Kunkel K, Santer B, Wehner M, Colle B, Fischer EM, Fu R, Goodman A, Janssen E, Kharin V, Lee H, Li WH, Long LN, Olsen SC, Pan ZT, Seth A, Sheffield J, Sun LQ. 2014. CMIP5 climate model analyses: climate extremes in the United States. Bull Am Meteorol Soc 95:571–83.

Yanai RD, Vadeboncoeur MA, Hamburg SP, Arthur MA, Fuss CB, Groffman PM, Siccama TG, Driscoll CT. 2013. From missing source to missing sink: long-term changes in the nitrogen budget of a northern hardwood forest. Environ Sci Technol 47:11440–8.

Young CL. 1981. Oxides of nitrogen. New York: Pergamon Press. p 388p.